Structural and Electronic Properties of Columnar Supramolecular Assemblies Formed from Ionic Metal Free Phthalocyanine on Au(111)

Krista R. A. Nishida, Bryan Wiggins, K. W. Hipps, and Ursula Mazur**
Department of Chemistry and Materials Science and Engineering Program, Washington State University, Pullman, Washington 99164-4630

Corresponding Author: e-mail: umazur@wsu.edu

ABSTRACT Highly ordered assemblies prepared from tetra (4-sulfonatophenyl) phthalocyanine, (TSPc), by employing very acidic aqueous solutions were deposited onto Au(111) substrates and studied in UHV using X-ray photoelectron spectroscopy (XPS), scanning tunneling microscopy (STM), and orbital mediated tunneling spectroscopy (OMTS). XPS of the TSPc aggregates shows that the ratio of protonated to unprotonated nitrogens does not change with decreasing solution pH. STM images of TSPc deposited from pH < 1 solutions reveal ordered branched web-like assemblies hundreds of nanometers in length, generally 2 nm tall and having variable widths. High-resolution UHV-STM images of TSPc aggregates on Au(111) reveal detailed coherent columnar architecture with the phthalocyanine macrocycles orientated parallel to the substrate surface. OMTS was used to identify high energy occupied orbitals and the LUMO of the TSPc aggregates and the results are contrasted with the same molecular states in unsubstituted metallated phthalocyanines (MPc). The positions of the filled and the empty states of the TSPc are comparable to those of other unsubstituted MPc's indicating that the electronegative sulfonate substituents have minimal effect on the electronic properties of the macrocycle in this aggregated state on Au. The HOMO-LUMO separation of the TSPc is slightly above 2 eV, a value consistent with the literature assignments for the Pc ring band gap.

(Rev 1: need 4,5 6: Rev 2: done—names, table, removed 12& fixed refs, X-ray etc,)

KEYWORDS: STM, OMTS, XPS, columnar aggregation, phthalocyanine

INTRODUCTION

Phthalocyanines (Pc) are one of the most studied functional molecular materials because they possess many useful physiochemical and optoelectronic properties.[1-10] To date, Pc's have served as building blocks for advanced photovoltaics,[2,5] sensors,[6] field-effect transistors,[7] nonlinear optics,[8] optical data storage,[9] and electrochromic displays.[10] These advanced technological applications, often require aggregated forms of the phthalocyanine for function, because the supermolecular Pc assemblies possess more advantageous physical, chemical, electrical, and optical properties than discrete molecular units.[1,10,11] Supramolecular Pc organization can be achieved through judicious manipulation of intermolecular interactions such as hydrogen bonding, electrostatic interactions, and π–π stacking. Cofacial columnar Pc assemblies, where the overlap between frontier molecular orbitals on adjacent molecules is maximized, are especially desirable for photovoltaic applications.[1,2,5] Such face-on molecular arrangements complemented by long range coherence ensures efficient charge and energy transport through the Pc columns to the external circuit.

Building aligned columnar Pc superstructures with coherence lengths several hundred nanometers in length is no easy task. Researches have tackled this structural design problem by employing both technology and chemistry in attempts to realize the desired molecular architecture. Longitudinal alignment of Pc columns from primarily alkoxy substituted metallated phthalocyanines (MPc) can be accomplished with Langmuir-Blodgett deposition,[10,12-16] spin casting,[15] and even spontaneous assembly.[17-19] Transverse orientation of Pc aggregates with the plane of the molecule aligned parallel to the substrate plane, an arrangement preferred for solar cell applications, is more difficult. Vapor deposition[20,21] and molecular beam epitaxy[22,23] of unsubstituted MPc achieved ordered multilayers with the plane of the molecule parallel to the substrate, however, ordering typically extended to only a few molecular layers. Chemically tailored phthalocyanines bearing hydrogen bonding groups within side chains[14,24] have shown promise in directing ordered aggregation in layer by layer deposition. In this type of aggregation, the kinetics of deposition must be carefully controlled and the choice of substrates is important, since the first monolayer acts as a template for the deposition of subsequent ones. Recently parallel alignment of the Pc rings on graphite and surface functionalized gold was

achieved by utilizing low concentrations of octylbenzamide ethyl-sulfanyl copper phthalocyanine.[24] This molecular system's extensive hydrogen bonding network produced ordered films, but only up to a maximum of 10 monolayers thick.

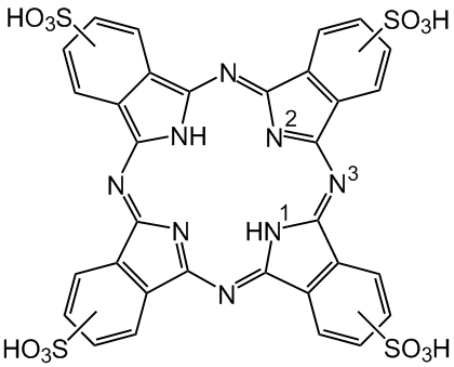

Figure 1. Molecular structure of phthalocyanine tetrasulfonic acid. TSPc has several regioisomers. Atom labels on the molecule refer to specific nitrogens in the XPS assignments discussed in this work.

Our approach for the growth of ordered vertical Pc assemblies is to use simple pH controlled processing technique employing free base phthalocyanine tetrasulfonic acid, TSPc, (Figure 1) to deposit cofacially coherent molecular columns with the Pc planes laying flat on a solid support. In this article, we report both spectroscopic and microscopic studies on self organization of TSPc, deposited from pH<1 solution on a Au(111) substrate. We employed low solution concentrations and short deposition times. Comparison of X-ray photoelectron spectra (XPS) of H_2Pc and TSPc powders with the TSPc aggregate indicates that in HCl solution (even at a pH as low as 0) no additional protonation of the ring nitrogens in the TSPc takes place. Images of the aggregates obtained by scanning tunneling microscopy (STM) in an ultra high vacuum environment provide the first 'topographical look' at the structure of vertical columnar phthalocyanine assemblies formed on a surface. We observed TSPc macrocycle planes aligned parallel to the gold surface forming stacks (5 molecules high) perpendicular to the substrate normal. Our STM derived dimensions for the Pc-Pc cofacial spacing agree very well with available X-ray diffraction (XRD) unit cell measurements for other H-bonded phthalocyanine assemblies.[24,25] The face to face stacking configuration of the TSPc aggregates results in the high degree of overlap between LUMO's on adjacent molecules and facilitates an efficient electron transport pathway – giving rise to an intense tunneling signal in the scanning tunneling spectra (STS) of the phthalocyanine. The effects of the sulfonate groups on the electronic properties of TSPc are also considered.

EXPERIMANTAL METHODS

Materials and Sample Preparation. The phthalocyanine tetrasulfonic acid, TSPc, was purchased from Frontier Scientific and used without further purification or separation of regioisomers. Free-abase phthalocyanine, H_2Pc, was acquired from Sigma-Aldrich. Gold metal, 99.999% pure was obtained from Cerac Co. All solvents and acids used were reaction grade. TSPc solutions were prepared in Millipore water (18 MΩ) previously degassed by boiling for 1 hour.

10μM aqueous solutions of TSPc at pH 5 and 0 were prepared using HCl for acidification at the lower pH. Au(111)/mica substrates prepared in-house were used in the XPS and SPM studies. The TSPc samples were deposited on Au(111) as follows. An aliquot of solution approximately 10μ was dropped directly onto the substrate, allowed to remain for approximately 10 min and then spun dry for 30 seconds at 4400 rpm.

Epitaxially grown Au(111) on mica substrates were used for XPS, STM, and OMTS studies. The Au films were prepared on mica by vacuum evaporation in a procedure similar to that used previously.[26] The evaporator was performed in a cryopumped chamber having a base pressure on the order of $5x10^{-10}$ Torr. The mica sheets (Ted Pella) were cleaved just before use with plastic tape. The substrate temperature was controlled by contact to a copper block heater. The temperature was monitored with an iron-constantan thermocouple and a millivolt meter giving an accuracy of about 2 °C. For most of the samples, mica substrates were first heated to 500 °C for 12 h at a pressure less than $2x10^{-9}$ Torr. The substrate was then cooled to 350 °C and maintained there during Au deposition. Gold (99.999%) was evaporated from a tungsten boat at a deposition rate of about 3 nm/min to form films with a thickness of roughly 150 nm. The pressure in the vacuum system prior to Au deposition was less than $8x10^{-10}$ Torr. The deposition rate was monitored with a thickness monitor (Sycon Instruments STM-100). Following gold deposition, the films were slowly cooled to below 30 °C in the vacuum. These films were either used immediately after preparation, or flame annealed in a hydrogen-oxygen flame before use.

UV-Visible. Electronic absorption spectra of 10 μM TSPc in acid solutions along with appropriate references were collected with Perkin-Elmer 330 and a Shimadzu UV-2501PC UV-visible spectrophotometers. 10mm quartz cuvettes were employed.

XPS. XPS samples of the TSPc aggregates were prepared with the same procedures as for the STM. TSPc and H_2Pc powder samples were pressed into indium shots. 280-300 watts of achromatic X-radiation at energy 1486.7 eV (monochromatic AlK_α) was used as XPS excitation

sources. The analyzer was set for a spatial resolution of 120 μm. The energy resolution was set to 1.0 eV for survey spectra, and to 0.15 eV for the higher resolution acquisitions of C1s, N1s, S2p, and Au4$f_{7/2}$ peaks. Binding energies were calibrated against the Au 4$f_{7/2}$ peak taken to be located at BE = 84.3 eV.

TSPc deposition methodology described previously yielded low to medium surface coverage of the gold substrates by aggregates producing satisfactory samples for SPM imaging. TSPc aggregate samples were stored in a vacuum desiccator. Samples were first examined by AFM and then were transferred to the STM instrument for further studies.

STM, dI/dV, and OMTS. Imaging experiments were performed in a UHV temperature controlled environment. The samples were transferred via air-lock into the UHV STM chamber (working pressure <1x10^{-10} Torr) where the TSPc aggregate samples were heated to 100-130°C for a period of 3 min or more in order to remove HCl and water. The STM and controller were purchased from RHK technology and both constant current images and I-V data were acquired with this system. Unless otherwise stated, the images were plane-fit and low-pass filtered. Most of the data was acquired at 19°C, but a few images and I-V curves were obtained from nanorods on Au(111) at 80K. Both etched W and $Pt_{0.8}Ir_{0.2}$ tips were used. Generally, the tips required a cleaning step (Argon ion sputtering) in order to produce high quality I(V) curves on a clean gold surface. Spectroscopy was performed by using the RHK software to measure current as a function of sample bias voltage, I(V), at fixed tip-sample separation (feedback off). Multiple curves were acquired at each setting and then averaged. dI/dV curves were obtained as a numerical derivative of the average I(V). Orbital mediated tunneling spectra, OMTS, (dI/dV at fixed height) were measured on well defined TSPc aggregates on Au(111).

RESULTS AND DISCUSSION

Aggregation of TSPc occurs both in solution and on the surface. Traditionally, one uses UV-Vis spectroscopy to monitor aggregation in solution, with blue (*H*-type) or red (*J*-type) shifts taken as indicative of the relative orientation of molecules within the aggregate. When the aggregate solution is used to form nanostructures on surfaces, the nanostructures may, or may not, be the same as the solution supported aggregates. First, the conventional solution phase

analysis based on UV-Vis data will be shown. N1s XPS spectra will then be used to probe the protonation state of the surface aggregates. Finally, STM and OMTS data will provide a detailed molecular picture of the nano-webs formed from pH 0 solution on Au(111).

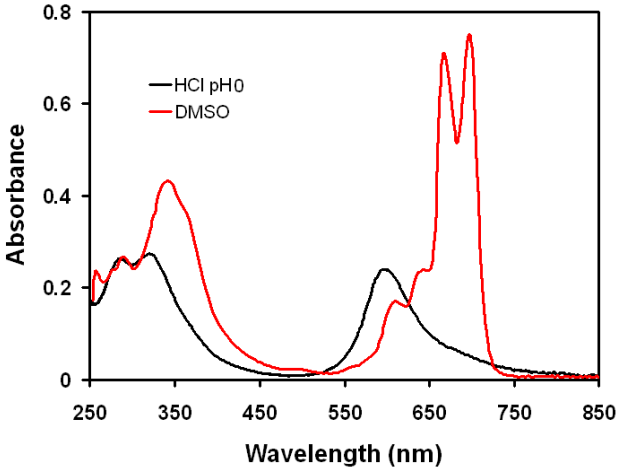

Figure 2. Absorption spectra (coded in color) of 10μM TSPc in water at pH 0 (black) adjusted with HCl. The red line spectrum is that of 10μM TSPc acquired in DMSO. This is a spectrum of monomeric phthalocyanine species presented here as a reference.

UV Visible spectra. Figure 2 contrasts the optical absorption spectrum of a 10 μM aqueous TSPc solution at pH 0 (aggregated) with that of the isolated molecule as seen in DMSO also at 10μM concentration. In DMSO, the metal-free phthalocyanine monomer species can be easily identified by the characteristic presence of two well-resolved intense Q_x and Q_y bands near 660 and 700 nm and two lower intensity vibronic transitions at 630 and 600 nm.[27,28] At pH 0 the Q-band blue shifts and significantly reduces in intensity. This type of spectral behavior, i.e. decreasing intensity and blue shifting of a broadened Q-band absorption is associated with aggregation of TSPc molecules in aqueous and high ionic strength solutions.[29-32] The aggregates formed are thought to be composed of two or more phthalocyanine units electronically coupled via π-π stacking or *H*-type aggregation. This idea was supported by the demonstration of CuTSPc dimers in dilute aqueous solutions as determined by small-angle X-ray scattering (SAXS) studies.[25] The long tailing of the Q-band suggests that single molecules may also be present. Any additional reduction in the intensity of the broadened Q-band is believed to be indicative of formation of higher order phthalocyanine aggregates.[33] Although the acid-base equilibrium constants for sulfonic acid substituents on the TSPc are not known, it is expected that the sulfonate groups remain ionized except in very acidic solutions.[34] For $-SO_3H$ groups in tetrasulfonylphenyl chlorin (a N_4-macrocycle related to a phthalocyanine), a pKa of 1.4 was estimated using Q-band absorbance titration curves.[35] By utilizing the same methodology we determined that the pKa for the dissociation of the $-SO_3H$ groups in TSPc in HCl to approximately equal 1.1, which is in very close agreement with the pKa found for the ionization

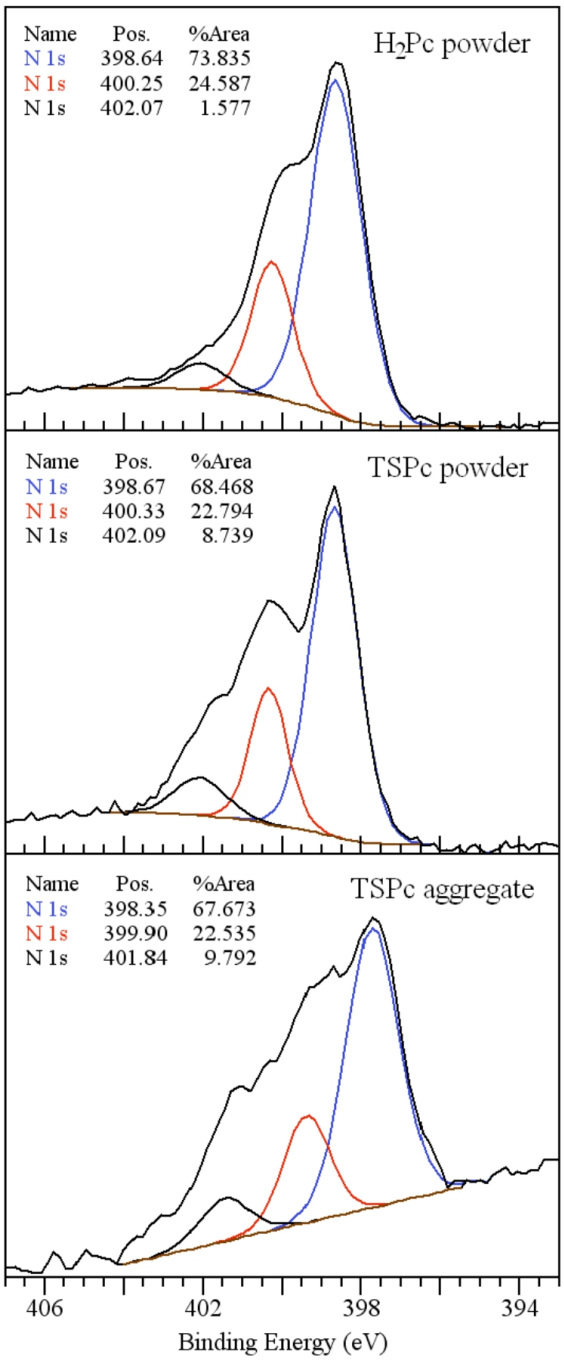

Figure 3. N1s region XPS for H_2Pc and TSPc powders and TSPc aggregates. The blue and red line fits in each spectrum are associated with the binding energies arising from the unprotonated and protonated Pc nitrogens, respectively. Black curve is a shake-up peak.

of sulfonate groups in the chlorin system.[35] Note that the p*K*a for the dissociation of the benzene sulfonic acid is 0.7.[36] Thus, it is reasonable to assume that in pH 0 solution all the sulfonate groups on the TSPc are protonated.

XPS. We performed XPS studies on Au(111) substrates treated with 0.75 M HCl, and those treated with 10 μM TSPc in 0.75M HCl. The Au(111) surface gave a clear but weak chlorine peak of about the same intensity was seen from HCl only and TSPc in HCl treated samples. When the samples were heated to ≥100°C in UHV, the chlorine signal disappeared. We interpret these results to mean that the Au is reacting with HCl to form a thin surface chloride layer that can be decomposed on heating. The N1s core-level spectra for the free base unsubstituted phthalocyanine, H_2Pc, and TSPc powders and the TSPc deposited from pH 0 solution on Au(111) are depicted in Figure 3.

All three spectra present three peaks with binding energies of 398, 400, and 402 eV. The two lower energy peaks originate from three nonequivalent nitrogen atoms in the molecule that are identified in Figure 1. The low intensity peak at 402.5 eV (black curve) is due to shake-up transitions. The peak near 398.6 eV (blue line fit) is associated with two types of coordinated nitrogens: the two pyrrole aza nitrogens, denoted as N2 in Figure 1, and the four

mesobridging aza nitrogens, denoted as N3. The binding energies of the two types of aza nitrogens lie very close together and usually are not resolvable.[37] The next peak at 400.4 eV (red line fit) is associated with two pyrrole nitrogens bonded to hydrogen atoms in the center of the molecule, denoted as N1 in the same figure. Our assignments of the binding N1s nitrogens in TSPc are consistent with previously reported XPS spectra of H_2Pc[38] and TSPc[37] complexes. Note that the in the spectrum of the TSPc aggregate adsorbed onto Au(111) the peak due to N3 and N2 shifts to lower binding energy by about 0.3 eV relative to the 398.67 eV signal from the same nitrogens in the bulk TSPc and H_2Pc (Figure 3). Similar lowering (by 0.4 eV) in the binding energy of the aza-nitrogens (N3 and N2) was observed in the XPS of CuTSPc absorbed from water onto surface oxidized multiwall carbon nanotubes, o-MWCNT.[39] This result was attributed to strong interaction between the phthalocyanines and the o-MWCNT substrate. Since the binding energy correlates with electron density around a nucleus, lowering in the binding energy of the azo N1s indicates that charge transfer occurs between the aggregated TSPc molecules and the gold surface. Another indicator for the interaction of the TSPc azo-nitrogens with the substrate is the broadening of the N1s manifold in comparison to the N1s spectrum of the bulk powder.

It is interesting to note that the binding energies of the nitrogens in the TSPc and the ratio of the unprotonated aza and pyrrole nitrogens (N2 and N3) to the hydrogen bearing nitrogens (N1) remain unaffected by the highly acidic environment from which the TSPc molecules were deposited on the Au(111). The ratio of the unprotonated to the protonated nitrogen atoms is 3:1 in all these species indicating that the pyrole nitrogens in the Pc are not protonated in HCl solution down to pH = 0. This is not the case for the tetrasulfonyl porphyrin, TSPP, which easily distorts to accommodate two additional protons in the macrocycle cavity under acidic conditions.[40,41] In a phthalocyanine, protonation at the inner isoindole-nitrogen atoms would cause a significant out-of-plane deformation of the macrocycle resulting in an energetically untenable conformation.[42] Outer protonation at the meso-nitrogen atoms is expected to be energetically more favorable than the inner protonation at the isoindole-nitrogen atoms. In fact, DFT calculations indicate that protonation of all the outer meso-nitrogen atoms produces the most stable Pc structure.[42] Protonation of the bridging aza nitrogens in a Pc can be achieved in highly concentrated H_2SO_4 solutions resulting in a red shift of the Q-band in the optical spectrum

of the macrocycle.[43,44] Both, our XPS and UV-vis experiments indicate that the TSPc bridging nitrogens do not protonate in HCl solutions at pH ≥ 0.

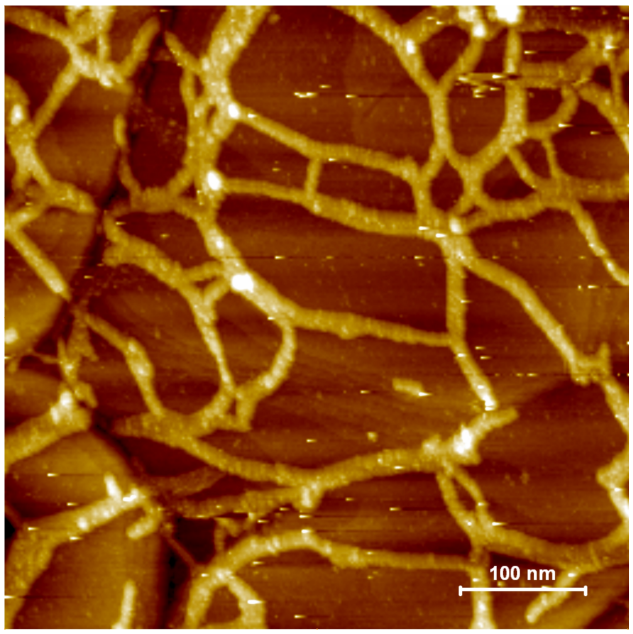

Figure 4. Large scale constant current STM image of TSPc aggregates on Au(111). Image was taken in UHV after heating the sample to 100º C. The set point was 1.6 V and 5 pA.

STM. A representative large scale STM image of TSPc aggregates formed on Au(111) acquired under UHV conditions is depicted in Figure 4. TSPc deposited from pH 0 solution forms web-like structures with branches that radiate predominantly at near 60° and 120° angles (perhaps following the structure of the gold substrate) and extend over the entire area of the substrate. Because the commercially acquired TSPc is composed of several regioisomers, the aggregates are not expected to propagate in a linear fashion. The dimensions of the aggregates, both height and width, vary but not widely: 1.6-2nm for the height and 20-60 nm for the width of the aggregates. The bodies of the aggregates remain intact upon repeated scanning without decomposing into TSPc molecules. We note that scanning under positive sample bias yielded clear STM images. With reverse bias it was difficult to obtain well resolved topography. This is indicative of primarily LUMO mediated tunneling.[45]

Higher resolution STM images of heated TSPc samples, shown in Figure 5, display branching aggregate filaments with nearly flat surfaces and well-defined edges. The edges in some aggregate filaments form graduated steps like the ones clearly visible in Figure 5b. A close inspection reveals that the filaments are composed of close lying parallel strands of molecules. In Figure 5a we observe different types of aggregate branches: one in which rows of TSPc molecules propagate down the length of the aggregate labeled 1 (the predominant form) and another in which parallel lines of molecules are aligned at nearly 60° to the long axis of the aggregate filament, labeled 2 (minor form). More detailed images of the form 2 aggregate are provided in the Supporting Information. Observe that the aggregate branches that extend from structure 2 in Figure 5a resume a molecular arrangement identified as structure 1 at the limb

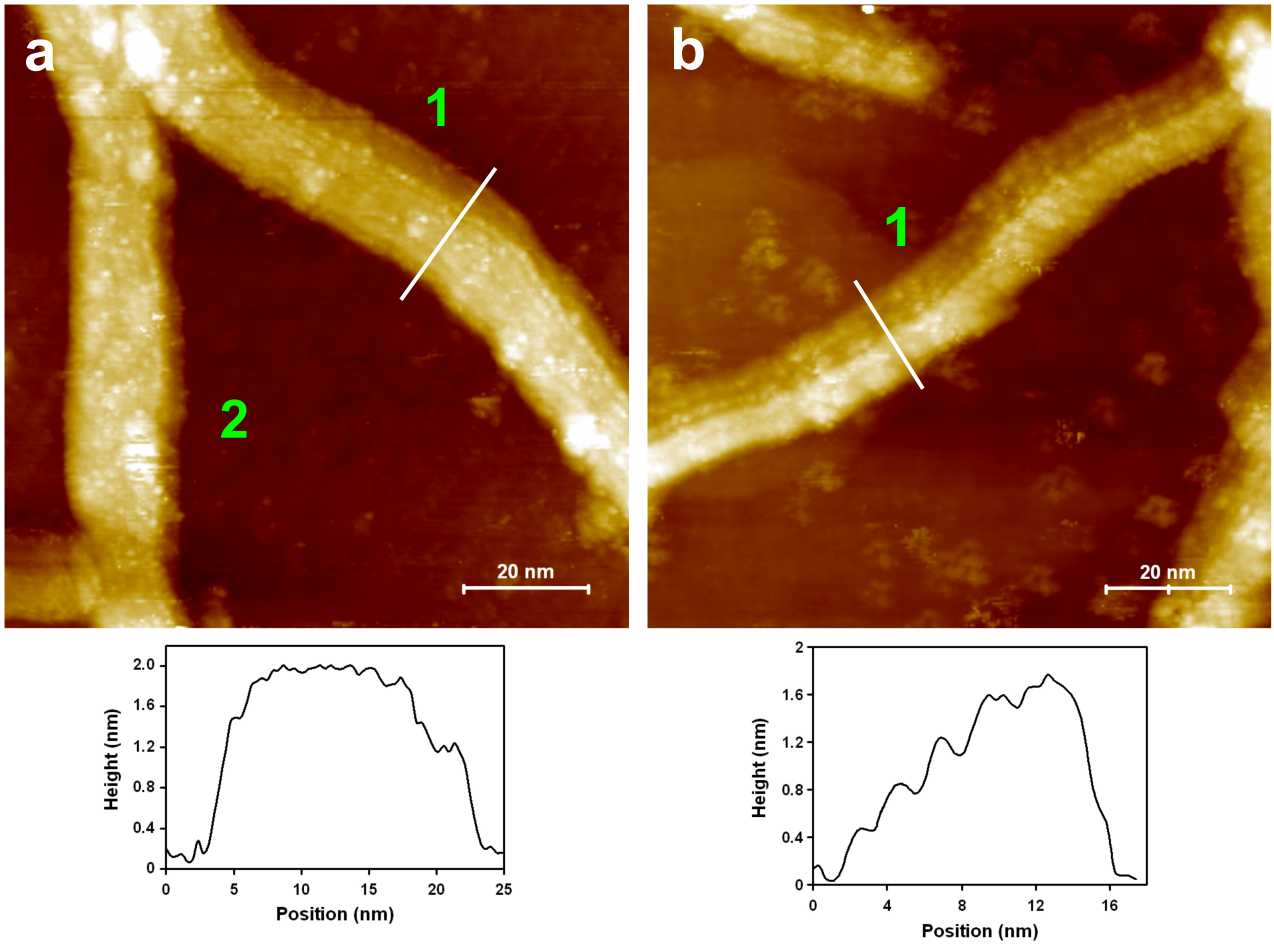

Figure 5. Representative UHV-STM images of TSPc aggregates formed on Au(111). Image (a) presents two types of self-organized structures: **1** parallel rows of TSPc molecules propagate down the length of the aggregate and **2** parallel lines of molecules are aligned at 60° to the long axis of the aggregate. In image (b) the parallel molecular rows form graduated steps. Both images were acquired after the samples were heated to 100 C. The set point was 1.6V and 5pA. Below each figure is a cross-section of a feature identified in the image.

junctures. At this time it is difficult to identify what drives this difference in structural behavior. It may be that we are seeing surface induced isomer separation. This conjecture, however, needs to be verified with images obtained from isomerically pure TSPc – a project currently underway in our laboratory. In the cross section associated with Figure 5b, the step height of the individual parallel molecular rows measures 0.4-0.5 nm and the width is about 2 nm. The staircase patterning of the TSPc molecules in 5b is not a multi-tip artifact. We have observed this type of structure in different TSPc aggregate samples imaged with different tips.

A clearer picture of the TSPc ordered assemblies on the gold surface emerges in the high-resolution image depicted in Figure 6. Here, the inter-row separation (2.0 ± 0.1 nm) is clearly

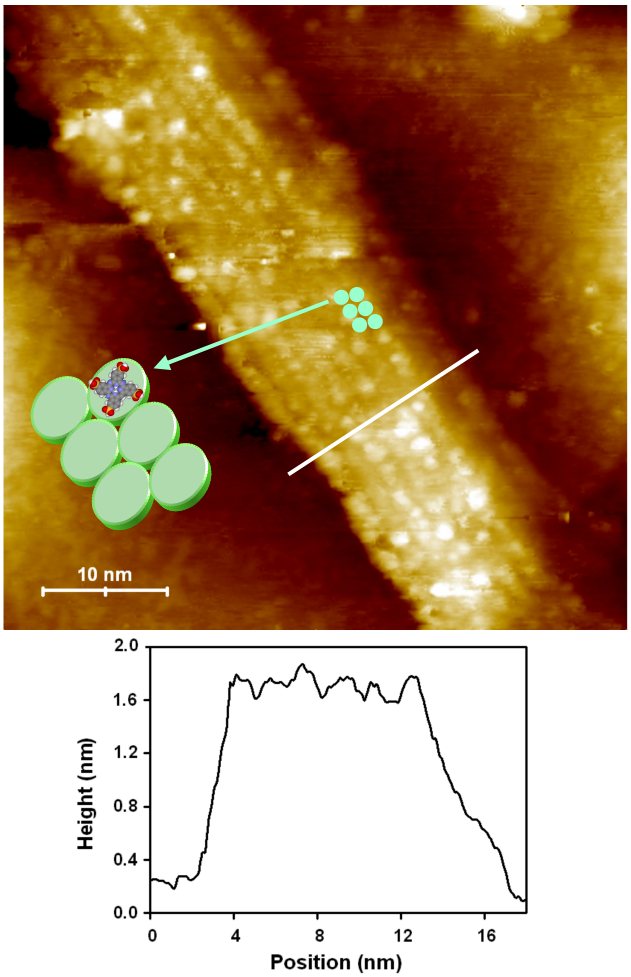

Figure 6. Constant current high resolution image of a TSPc aggregate along with a cross-sectional view of molecular packing of the phthalocyanine. The sample was heated to 100 C in UHV before imaging. The molecular rows are 2 nm apart. The set point was 1.6V and 5pA.

identifiable and well documented by the cross-sectional profile of the aggregate filament. The widths of the molecular rows are approximately the same as the diameter of individual TSPc molecules, namely ~2 nm. The separation between molecules within a row is 1.7 ± 0.2 nm. This value is in excellent agreement with a wide angle X-ray diffraction (WAXD) pattern of CuTSPc molecules crystallized in solvated polycationic gels, where the phthalocyanine formed hexagonal columns separated by a distance of 1.72 nm.[25] To our knowledge, there are no single-crystal structures reported for pure TSPc based compounds. Note that the top of the filament is incredibly flat and its sides are very steep giving the aggregate a rectangular form. Such restrained geometry implies a high level of ordering of molecules in all three dimensions.

The structural evidence presented in figures 5 and 6 can only result from self-assembly of the TSPc macrocycles with the Pc planes aligned perfectly parallel to the gold surface forming stacks perpendicular to the substrate normal. The measured vertical TSPc-TSPc separation is 0.45nm, which is consistent with eclipsed cofacial π-π arrangement of the macrocycles dictated by H-bonding of protonated sulfonate groups between the Pc rings. A similar value for the Pc-Pc cofacial spacing was reported in X-ray diffraction studies of other H-bonded phthalocyanine assemblies with large ring substituent.[19,24] For example, a XRD study of self-organized 2,3,9,10,16,17,23,24-octa(2-(4-octylbenzamide ethyl-sulfanyl) phthalocyanine films on amine modified gold substrates reported a columnar aggregate with Pc layer planes

separated by multiples of 0.4-0.5 nm consistent with hydrogen-bonding interaction.[24] An AFM cross sectional analysis of this film indicated that the average layer thickness was 0.44 nm; however, no molecular resolution was achieved.[24] SAXS studies of CuTSPc aggregates in dilute aqueous solutions (2.00 - 0.25 weight % Pc) also measured a distance of 0.5 nm between the planes of Pc dimers.[25]

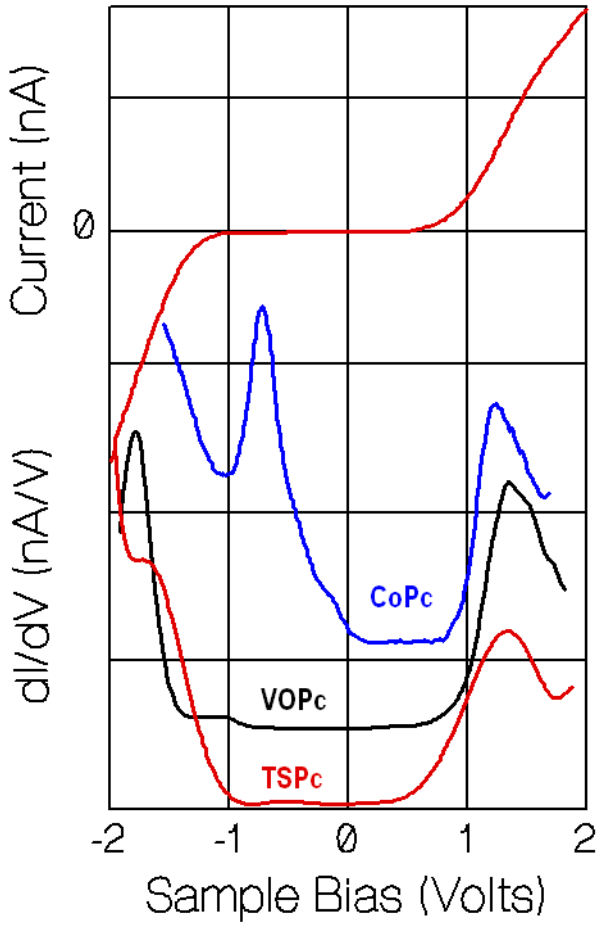

Figure 7. Comparison of area averaged d*I*/d*V* spectra taken from a TSPc aggregate (red trace) with those obtained from monolayer films of CoPc (blue trace, reference 48) and VOPc (black trace, reference 47) all on Au(111). The zeros of each trace are placed arbitrarily to allow easier comparison of spectra. Also shown is the *I/V* curve obtained from three layers of TSPc on Au(111).

Our STM data provides the first molecular level microscopic evidence for columnar assemblies of phthalocyanines formed on surfaces. The dimensions associated of these structures are in good agreement with XRD data obtained for other π-π stacked phthalocyanines. While most single-crystal and thin film derived discotic assemblies exhibit some tilt of the Pc's within columns, the TSPc aggregates deposited from pH 0 form perfect face-on aligned columns at least five molecules thick.

We have learned that a very low pH environment is necessary for protonating the sulfonate groups, thereby initiating H-bonding that aligns the TSPc columns. Higher pH conditions (>1) proved less effective for producing ordered TSPc assemblies and results of that work will be reported elsewhere.

I/V curves and OMTS. We interpret the spectra in Figure 7 in terms of orbital mediated tunneling, OMT.[45,46,47] In addition to the TSPC aggregate OMTS trace, we have included the tunneling spectra of CoPc[46,48-50] and VOPc[47] monolayers (reported earlier) for comparison. The

intense peak near +1.35 eV in the TSPc tunneling spectrum is attributed to tunneling mediated by the π^* LUMO of the Pc ring and the same peak occurs in essentially the same place for all three phthalocyanines shown. The complex of peaks seen between 0 and -1 V bias in the CoPc spectrum are attributed to a superposition of both the half-filled d_{z^2} orbital of the cobalt(II) ion and to the HOMO of the phthalocyanine ring. The intense peak (or shoulder) seen in all three spectra near -1.75 V we attribute to HOMO-1 and HOMO-2 (a nearly degenerate pair). The intensity of the HOMO-1 and HOMO-2 peaks of TSPc, are consistent with the analysis and of the STM image of H_2Pc presented by Nilson.[51]

The very weak or absent HOMO peak is a bit of a mystery. Why is the band near -0.7 V bias so strong in CoPc and not clearly seen in VOPc or in the TSPc aggregate (also by implication in H_2Pc[51]). The same HOMO band is clearly present in naphthalocyanine on HOPG.[52] We can suggest two possibilities and we realize there may be other alternatives. In the first scenario, there is significant mixing of metal and π HOMO in the case of CoPc. To support this, recent XPS, UPS, and X-ray Excited Auger Electron Spectroscopy (XAES) studies provided evidence for a negative charge transfer at the CoPc/Au(111) interface from the substrate into the molecule facilitated by a considerable coupling between the d orbitals of the Co ion and the gold metal surface states.[53,54] Moreover, the image of monolayer and multilayer CoPc is well known to reflect mixing between the metal substrate and cobalt ion.[45,48,49,55] Mixing of metal orbitals and HOMO, when combined with the known Co-Au interaction of the adsorbed CoPc, may result in significantly enhanced tunneling through the HOMO. In the absence of this indirect mixing with Au states, the HOMO tunneling intensity may be weak. Thus, in the case of H_2Pc and TSPc, where there is no central metal to strongly interact with the substrate, the HOMO does not play a significant role in the elastic tunneling. In the VOPc case, the strong covalent link between V and O, and the displacement of the vanadium from the center of the molecule, also result in poor vanadium-gold mixing and thus a weak HOMO band. Left unanswered in this picture, is why the HOMO tunneling is intrinsically weak.

An alternative picture accounts for the TSPc aggregate case, but not for VOPc. In the alternative picture, it is recognized that the tunneling current observed must pass through several TSPc layers. Thus, one can observe only those orbitals with high individual tunneling rates and having significant overlap with the same orbitals on adjacent molecules. The extreme view here is that some of the current may be due to conduction at bias voltages above and below the

HOMO-1/LUMO band gap. It needs to be stressed that in the preceding discussion we were comparing the spectral results obtained for the CoPc and VOPc monolayers with *dI/dV* for TSPc cofacially stacked aggregate layers ~2 nm high. We are therefore, measuring transverse conductivity through columns five molecules thick. Since the LUMO of the TSPc is mainly due to the macrocycle's affinity states, the co-facially stacked configuration is expected to result in the highest degree of overlap between LUMO's on adjacent molecules and facilitate efficient electron transport.

We turn to two different approaches to justify our assertion that the HOMO and LUMO positions of TSPc are essentially the same as those for H_2Pc. The first argument relates to the relative ineffectiveness of the electron withdrawing effect created by the sulfonates. The second argument relies upon *ab-initio* DFT calculations.

Why do the electron withdrawing sulfonate groups appear to have no effect on the positions of the molecular orbitals? Recent tunneling studies showed that there is a small shift (0.2 V) to lower energy in both HOMO and LUMO of perfluorinated CoPc ($CoF_{16}Pc$) and $CuF_{16}Pc$ monolayers on gold or silver relative to the parent CuPc and CoPc.[56-58] However, the HOMO/LUMO edges of $Cl_{16}CuPc$[56] shifted only marginally. The HOMO edge of $CuF_{16}Pc$ adsorbed on Au(111) shifted to higher energy by +0.22 eV, while the LUMO moved by ~ +0.4 eV compared to the same levels in CuPc relative to the vacuum level.[56] The positions of first ionization and electron affinity states for a series of symmetrically substituted, CoF_4Pc, CoF_8Pc, and $CoF_{16}Pc$ adsorbed on Ag(110) also exhibited a similar systematic but small shift toward higher energies compared to the HOMO and LUMO for the parent CoPc molecule.[57] All these tunneling results were consistent with UPS measurements of the ionization potentials on the same systems.[48,53,59] UPS combined with inverse photoemission spectroscopy (IPES) was employed to compare the electronic structure of CuPc, Cu F_8Pc, and Cu $F_{16}Pc$ adsorbed on gold. This study produced results in excellent agreement with the OMTS findings.[59] Interestingly, both the OMTS[56,57] and UPS-IEPS[59] works measured a constant transport gap energy at 2.0± 0.1 eV for all the halogenated phthalocyanines investigated. We here assert that the HOMO-LUMO gap in the TSPc aggregate also has a comparable band gap of about 2.0 eV. We believe this is for two reasons. First, we should not expect the four sulfonate substituents to have the same profound effect on the electronic structure of the phthalocyanine as the more electronegative fluorine substitution, considering that the $CuCl_{16}Pc$[56] monolayer exhibited an OMTS very similar

to that of the CuPc complex. To get a better feel for implication of electronegative substituents on the HOMO/LUMO energies of phthalocyanines it is convenient to take advantage of the Hammett constant (σ),[60,61] which correlates well with the redox potentials (ionization potential and electron affinity, EA) for substituted MPc in solution. Using the relevant MPc σ and redox values from the literature we obtain the following trend: H_2Pc (σ = 0,[60] EA = 4.01 eV[60]), TSPc(σ = 1.4,[60] EA = 4.18 eV[60]), Fe($Cl_{16}Pc$) (σ = 3.68,[60] EA = 4.22[62]) Co($F_{16}Pc$) (σ = 7.68,[61] EA = 4.36[63]). The solution phase electron affinity (EA) values were obtained by equating the reported reference SCE potential to 4.71 eV relative to the vacuum level.[41,45] In this grouping of phthalocyanines, it is quite apparent that four sulfonate groups, having a σ value of less than 20% of that for $F_{16}Pc$, will exert only a weak effect on the electron affinity level of the Pc. Thus, it is not surprising that the TSPc adsorbate HOMO-LUMO split remains invariant.

An alternative approach to justifying the constancy of band gap in the parent and sulfonated phthalocyanines is to use a DFT calculation using the B3LYP functional and the 6-31g+(d,p) basis. All calculations were performed for the gas phase molecules and the structures were optimized. We note, however, that the barrier to rotation of the sulfonate groups is so low that there is little difference in total energy for the case of two OH groups up and two down, or for one OH group up and three down. We calculated the barrier to rotation of one sulfonate in the pseudo C_{2h} isomer of H_4TSPc to be only 3.3 kcal/mole. In addition to considering the effects of SO_3H group rotation on the energy, we also considered the structural isomers by performing the calculation on two of the four possible structures,[64] the pseudo C_{2h} and the C_s structures. Consideration of the results reported in Table 1 clearly demonstrates that the orbital splitting of the ligand orbitals near the HOMO and LUMO is essentially the same out to a few hundredths of an eV.

One does notice that the calculations give different relative zero's of energy, with the gas phase H_4TSPc levels laying about 1 eV deeper than those calculated for gas phase H_2Pc. Why then are the levels of the two species so similar when supported on Au? One possibility is that presented by Toader and co-workers.[57] They postulate that the "molecular Fermi energy" is mid band gap and that the substrate and molecular Fermi energies equilibrate. A less specific but perhaps more accurate description would take into account the local potential experienced by the adsorbate and charge redistribution afforded by condensed phase hydrogen bonding. Experimentally, it is clear that the LUMO of TSPc is not shifted from +1.35 to +0.35 V (as

suggested by gas phase calculations), but rather is within a few hundredths of an eV for both molecular systems.

Table 1. Calculated symmetry and energies for H_2Pc orbitals and energies for H_4TSPc in both high symmetry and C_s isomer forms. The last column is the difference between the orbital energy in H_2Pc and the pseudo C_{2h} symmetry H_4TSPc isomer. The solid line separated occupied and virtual orbitals.

Symmetry C_{2h} [a]	-E[b] H_2Pc	-E+0.0386[b] H_4TSPc	-E+0.0376[b] C_s H_4TSPc	(eV) H_2Pc	Δ (eV)+1.050 H_4TSPc
A_u	0.0529	0.0604	0.0598	-1.44	0.20
B_g	0.1142	0.1137	0.1138	-3.11	-0.01
B_g	0.1157	0.1157	0.1157	-3.15	0.00
A_u	0.1937	0.1935	0.1935	-5.27	-0.01
A_u	0.2508	0.2511	0.2512	-6.82	0.01
B_g	0.2519	0.2537	0.2538	-6.85	0.05
A_u	0.2613	0.2615	0.2616	-7.11	0.01
B_g	0.2633	0.2642	0.2640	-7.16	0.02
A_u	0.2670	0.2677	0.2678	-7.26	0.02
B_g	0.2701	0.2697	0.2703	-7.35	-0.01
B_g	0.2715	0.2714	0.2714	-7.38	0.00
A_g	0.2745	0.2714	0.2716	-7.47	-0.08
A_u	0.2756	0.2739	0.2746	-7.50	-0.05
B_u	0.2856	0.2826	0.2827	-7.77	-0.08

[a]Symmetry of orbitals for H_2Pc having C_{2h} geometry. [b]Energy in Hartrees.

CONCLUSIONS

We have demonstrated a simple pH controlled processing technique for growth of ordered assemblies of ionic TSPc molecules on a gold substrate. TSPc deposited from pH 0 solution acidified with HCl, forms web-like structures with branches that radiate predominantly along the symmetry directions of the gold substrate and extend over the entire area of the substrate. Our high resolution STM data provide the first single-molecule level microscopic evidence for the formation of columnar phthalocyanine assemblies on a surfaces. Here the TSPc macrocycle planes are aligned parallel to the gold surface forming stacks (5 molecules high) perpendicular to the substrate normal. The measured vertical TSPc-TSPc separation is 0.45nm, which is consistent with eclipsed cofacial π-π arrangement of the macrocycles dictated by H-bonding of

protonated sulfonate groups between the Pc rings. Our STM derived dimensions for the Pc-Pc cofacial spacing agree very well with available XRD unit cell measurements for other H-bonded phthalocyanine assemblies.

Comparison of the OMTS of non-sulfonated Pcs with that of TSPc clearly shows that surface and molecule-molecule interactions significantly reduce the electron withdrawing effects associated with the sulfonate substitution predicted in the gas phase. Moreover, a comparison of the DFT orbitals for H_6TSPc and for H2Pc demonstrates that the difference in gas phase energies for the higher occupied and lower unoccupied orbitals is almost exclusively a static 1.05 eV shift. Thus, image charges in the metal substrate and dielectric shielding can bring the HOMOs and LUMOs of these compounds into close allignment.

XPS results indicate that the binding energies of the nitrogens in the TSPc aggregates remain unaffected by the highly acid environment from which they were deposited. The ratio of the unprotonated to protonated nitrogen atoms in the H_2Pc and TSPc powders is the same and remains unchanged in the TSPc aggregate indicating that the pyrole nitrogens in the Pc are not protonated in HCl solution, even at a pH as low as 0. This is an important contributing factor to the H-aggregation displayed by these molecules. By contrast, in porphyrin systems at this pH protonation of all four inner nitrogen leads to strong deformation from a planar structure and elecectrostatic repulsion that results in J-aggregation.

The electron affinity and the ionization potential energies for 2 nm thick TSPc molecular stacks deposited on the Au(111) are very nearly identical to the HOMO and LUMO positions of unsubstituted phthalocyanines indicating that the four sulfonate substituents have little effect on the electronic structure of the phthalocyanine. The cofacial stacking configuration of the TSPc aggregates results in a high degree of overlap between LUMO's on adjacent molecules and facilitates efficient electron transport – giving rise to an intense tunneling signal. The very weak first ionization (HOMO OMTS) band is likely due to the HOMO being less effective in providing a path for electron transfer through the stack If the HOMO mediated transfer between a single pair of TSPc is 70% of that of the LUMO, the net transfer efficiency through a stack of five TSPc would be 17% or less relative to the LUMO.

We have demonstrated that a simple pH controlled deposition of ionic phthalocyanines eliminates the need for either long chain functionalities and/or chemically modified substrates to promote cofacial self-assembly and stabilization of phthalocyanine stacks on solid supports. At

this point, however, this technique also yields only a limited stack (about 5 molecules), and does not provide uniform coverage. It is possible, however, that a change in substrate and deposition conditions might result in more uniform coverage.

ACKNOWLEDGMENT This material is based upon work supported by the National Science Foundation under grants CHE-0848511, CHE-1048600, and CHE-1058435.

Supporting Information Available: UHV-STM images of TSPc aggregates showing molecular row orientation relative to growth direction. This material is available free of charge via the Internet at http://pubs.acs.org.

REFERENCES AND NOTES

[1] Liu, J-Y. Lo, P-C.; K.P. Ng, D. K. P. Phthalocyanine-containing supramolecular arrays. *Struct. Bond.* **2010**, *35*, 169–210.

[2] de la Torre, G.; Bottari, G.; Torres, T. Functional phthalocyanines: synthesis, nanostructuration, and electro-optical applications. *Struct. Bond.* **2010**, *135*, 1–44.

[3] Zhang, Y.; Cai, X.; Bian, Y.; Jiang, J.. Organic semiconductors of phthalocyanine compounds for field effect transistors (FETs). *Struct. Bond.* **2010**, *135*, 275-322.

[4] Mack, J.; Kobayashi, N. Low symmetry phthalocyanines and their analogues. *Chem. Rev.* 2**011**, *111*, 281-321.

[5] Martinez-Diaz, M. V.; de la Torre, G.; Torres, T.. Lighting porphyrins and phthalocyanines for molecular photovoltaics**.** *Chem. Commun.* **2010**, *46*, 7090-7108.

[6] Elemans, J. A. A. W.; van Hameren, R.; Nolte, R. J. M.; Rowan, A.E. Molecular materials by self-assembly of porphyrins, phthalocyanines, and perylenes. *Adv. Mater.* **2006,** *18*, 1251.

[7] Karimov, Kh. S.; Saleem, M.; Mahroof-Tahir, M.; Khan, T. A.; Khan, A. Pressure sensitive organic field effect transistor. *Physica E* **2010**, *43,* 547-551.

[8] Chen, Y.; Hanack, M.; Blau, W.J.; Dini, D.; Liu, Y.; Lin, Y.; Bai, J. Soluble axially substituted phthalocyanines: synthesis and nonlinear optical response. *J. Mat. Sci.* **2006**, *41*, 2169–2185.

[9] Di Bella, S.; Dragonetti, C.; Pizzotti, M.; Roberto, D.; Tessore, F.; Ugo, R.. Coordination and organometallic complexes as second-order nonlinear optical molecular materials. *Top. Organomet. Chem.* **2010**, *28*, 1-55.

[10]Armstrong, N. R.; Wang, W.: Alloway, D. M.; Placencia, D.; Ratcliff, E.; Brumbach, M. Organic/organic heterojunctions: organic light emitting diodes and organic photovoltaic devices. *Macromol. Rapid Commun.* **2009**, *30*, 717–731.

[11] Martinez-Diaz, M.V.; Bottari, G. Supramolecular organization of phthalocyanines: from solution to surface. *J. Porph. Phthal.* **2009**, *13*, 471-480.

[12] Oshiro, T.; Backstrom, A.; Cumberlidge, A. M.; Hipps, K. W.; Pevovar, S. P.; Bahr, D. F.; Smieja, J.; Mazur, U. Nanomechanical properties of ordered phthalocyanine Langmuir–Blodgett layers. *J. Mater. Res.* **2004**, 19, 1462-1470.

[13] Smolenyak, P.; Peterson, R.; Nebesny, K.; Torker, M.; O'Brien, D. F.; Armstrong, N. R. Highly ordered thin films of octasubstituted phthalocyanines. *J. Am. Chem. Soc.* **1999**, *121*, 8628–8636.

[14] Minch, B., A.; Xia, W.; Donley, C. L. Hernandez, R. M.; Carter, C.; Carducci, M. D.; Dawson, A.; O'Brien, D. F.; Armstrong N. R.; Octakis(2-benzyloxyethylsulfanyl) copper (II) phthalocyanine: A new liquid crystalline discotic material with benzyl-terminated, thioether-linked side chains. *Chem. Mater.* **2005***, 17,* 1618-1627.

[15] Ingrosso, C.; Curri, M. L.; Fini, P.; Giancane, G.; Agostiano, A.; Ludovico Valli, L. Functionalized copper(II)-phthalocyanine in colution and as thin film: photochemical and morphological characterization toward applications. *Langmuir* **2009**, *25*, 10305–10313.

[16] Nakanishi, T. Langmuir-Blodgett (LB) films on electrodes (B) electrochemistry. *Encycloped. Electrochem.* **2007,** *11,* 203-210.

[17] Kimura, M.; Muto, T.; Takimoto, H.; Wada, K.; Ohta, K.; Hanabusa, K.; Shirai, H.; Kobayashi, N. Fibrous assemblies made of amphiphilic metallophthalocyanines. *Langmuir* **2000,** *16,* 2078-2082.

[18] Bertoncello, P.; Peruffo, M. An investigation on the self-aggregation properties of sulfonated copper(II) phthalocyanine (CuTsPc) thin films *Colloids Surf. A* **2008**, *32,* 106–112.

[19] Duzhko,V.; Du, J.; Zorman, C. A.; Singer, K. D. Electric field patterning of organic nanoarchitectures with self-assembled molecular fibers. *Phys. Chem Lett.* **2008,** *112,* 12081–12084.

[20] Barlow, D.; Scudiero, L.; Hipps, K. W. Scanning tunneling microscopy of 1, 2, and 3 layers of electroactive compounds. *Ultramicroscopy* **2003**, *97,* 47-53.

[21] Hooks, D. E.; Fritz, T.; Ward, M. D. Epitaxy and molecular organization on solid substrates. *Adv. Mater.* **2001**, *13*, 227-241.

[22] Walzer, K.; Toccoli, T.; Pallaoro, A.; Iannotta, S.; Wagner, C.; Fritz, T.; Leo, K. Comparison of organic thin films deposited by supersonic molecular-beam epitaxy and organic molecular-beam epitaxy: The case of titanyl phthalocyanine. *Surf. Sci*. **2006**, *600*, 2064–2069.

[23] Schafer, A. H.; Seidel, C.; Fuchs, H. LEED and optical spectroscopy study of an organic epitaxial multilayer film. *Adv. Funct. Mater.* **2001**, *11*, 193-197.

[24] Kumaran, N.; Veneman, P. A.; Minch, B. A.; Mudalige, A.; Pemberton, J. E.; O'Brien, D. F.; Neal R. Armstrong, N. R. Self-organized thin films of hydrogen-bonded phthalocyanines: characterization of structure and electrical properties on nanometer length scales. *Chem. Mater.* **2010**, *22*, 2491–2501.

[25] Shimode, M.; Urakawa, H.; Yamanaka, S.; Hoshino, H.; Harada, N.; Kajiwara, K. Evaluation of size and shape of copper phthalocyanine tetrasulphonic acid tetra sodium salt and C. I. Reactive Blue 19 in aqueous solution. *Sen'i Gakkaishi* **1996**, *52*, 293-300.

[26] Hipps, K. W.; Lu, X.; Wang, X. D.; Mazur, U. Metal d-orbital occupation-dependent images in the scanning tunneling microscopy of metal phthalocyanines *J. Phys. Chem.* 1996, *100*, 11207-11210.

[27] Schlettwein, D.; Oekermann, T.; Yoshida, T.; Tochimoto, M.; Minoura, H. Photoelectrochemical sensitization of ZnO-tetrasulfophthalocyaninatozinc composites prepared by electrochemical self-assembly. *J. Electroanal. Chem.* **2000**, *481*, 42-51.

[28] Mack J.; Stillman, M.J. Electronic structures of metal phthalocyanine and porphyrin complexes from analysis of the UV-visible absorption and magnetic circular dichroism spectra and molecular orbital calculations. *Porph. Handbook: Phthal. Electrochem. Charac*. **2003**, *13*, 43-116.

[29] Lebedeva, N. Sh. Aggregation properties of water-soluble metal phthalocyanines: effect of ionic strength of solution. *Russ. Chem. Bull. Internat. Ed.* **2004***, 53,* 2674-2683.

[30] Kobayashi, N.; Lever, A. B. P. Cation or solvent-induced supermolecular phthalocyanine formation: crown ether substituted phthalocyanines. *J. Am. Chem. Soc.* **1987,** *109,* 7433-7441.

[31] Kroon, J. M.; Koehorst, R.B.M.; van Dijk, M.; Sandersa, G. M.; Sudholter, Self-assembling properties of non-ionic tetraphenylporphyrins and discotic phthalocyanines carrying oligo(ethylene oxide) alkyl or alkoxy units. E. J. R. *J. Mater. Chem.* **1997**, *7*, 615–624.

[32] Camp, P. J.; Jones, A. C.; Neely, R. K.; Speirs, N. M. Aggregation of copper(II) tetrasulfonated phthalocyanine in aqueous salt solutions. *J. Phys. Chem. A* **2002,** *106,* 10725-10732.

[33] Kasuga, K.; Yashiki, K.l Sugimori, T.; Handa, M. Bathochromic shift of the Q-bands of octakis(p-t-butylbenzyloxy)phthalocyanine with magnesium(II), nickel(II), and copper(II) in a solvent mixture and acetic acid. *J. Porph. Phthal.* **2005**, *9*, 646-650.

[34] Simic-Glavaski, B.; Zecevic, S.;Yeager, E. Spectroscopic and electrochemical studies of transition-metal tetrasulfonated phthalocyanines. 3. Raman scattering from electrochemically adsorbed tetrasulfonated phthalocyanines on silver electrodes. *J. Am. Chem. Soc.* **1985,** *107,* 5625-5635.

[35] Kruk. M. M.; Braslavsky S. E. Acid-base equilibria in 5,10,15,20-tetrakis(4-sulfonatophenyl)chlorin: Role of conformational flexibility. *J. Phys. Chem. A* **2006**, *110,* 3414-3425.

[36] Serjeant, E. P., and Dempsey, B. *Ionization Constants of Organic Acids in Aqueous Solution*. Pergamon, Oxford, 1979. ISBN-10: 0080223397

[37] Zhao, P.; Niu, L.; Huang, L.; Zhangz, F. Electrochemical and XPS investigation of phthalocyanine oligomer sulfonate as a corrosion inhibitor for iron in hydrochloric acid. *J. Electrochem. Soc.* **2008***, 155*, C515-C520.

[38] Alfredsson, Y.; Brena, B.; Nilson, K.; Åhlund, J.; Kjeldgaard, L.K.; Nyberg, M.; Y. Luo, Y.; Mårtensson, N.; Sandell, A.; Puglia, C.; Siegbahna, H. Electronic structure of a vapor-deposited metal-free phthalocyanine thin film**.** *J. Chem. Phys.* **2005**, *122,* 214723 -214725.

[39] Hatton, R. A.; Blanchard, N. P.; Stolojan, V.; Miller, A. J.; Silva, S. R. P. Nanostructured copper phthalocyanine-sensitized multiwall carbon nanotube films. *Langmuir* **2007**, *23,* 6424-6430.

[40] Friesen, B.A.; Nishida, K. R. A.; McHale, J. L.; Mazur, U. New nanoscale insights into the internal structure of tetrakis(4-sulfonatophenyl) porphyrin nanorods. *J. Phys. Chem. C* **2009**, *113*, 1709-1718.

[41] Friesen, B. A.; Wiggins, B.; McHale, J. L.; Mazur, U.; Hipps, K. W. A self-assembled two-dimensional zwitterionic structure: H_6TSPP studied on graphite. *J. Phys Chem. C* **2011**, *115,* 3990-3999.

[42] Lu, T-T.; Xiang, M.; Wang, H-L.; He, T-J.; Dong-Ming Chen, D-M. Density functional theory studies of N-protonation of the free base phthalocyanine. *J. Molec. Struct.: Theochem.* **2008**, *860*, 141–149.

[43] Lee, H. W. H.; Huston, A. L.; Gehrtz, M.; Moerner, W. E. Photochemical hole-burning in a protonated phthalocyanine with gallium aluminum arsenide diode lasers. *Chem. Phys. Lett.* **1985**, *114*, 491-506.

[44] Petrik, P.; Zimcik, P.; Kopecky, K.; Musil, Z.; Miletin, M.; Loukotova, V. Protonation and deprotonation of nitrogens in tetrapyrazinoporphyrazine Macrocycles. *J. Porph. Phthal.* **2007**, *11*: 487-495.

[45] Hipps, K. W. Scanning tunneling spectroscopy, in *Handbook of Applied Solid State Spectroscopy*, Ed: Vij, D. R., Springer Verlag **2006** ISBN: 0-387-32497-6.

[46] Barlow, D. E. ; L. Scudiero, L.; Hipps, K. W. Scanning tunneling microscopy study of the structure and orbital-mediated tunneling spectra of cobalt(II) phthalocyanine and cobalt(II) tetraphenylporphyrin on Au(111): Mixed composition films. *Langmuir* **2004,** *20,* 4413-4421.

[47] Hipps, K. W.; Barlow, D. B.; Mazur, U. Orbital mediated tunneling in vanadyl phthalocyanine observed in both tunnel diode and STM environments. *J. Phys. Chem. B* **2000,** *104,* 2444-244.

[48] Gyarfas, B.; Wiggins, B.; Hipps, K. W. Temperature independence of orbital mediated tunneling in cobalt(II) phthalocyanine. *J. Phys. Chem. C* **2010**, *114*, 13349-13353.

[49] Lu, X., Hipps, K.W.; Wang, X. D.; Mazur, U. Scanning tunneling microscopy of metal phthalocyanines: d^7 and d^9 cases. *J. Am. Chem. Soc.* **1996**, *118*, 7197-7202.

[50] Scudiero, L.; Hipps, K. W.; Barlow, D. E. A self-organized two-dimensional bimolecular structure. *J. Phys. Chem. B* **2003,** *107,* 2903-2909.

[51] Nilson, K.; Ahlund, J.; Brena, B.; Gothelid, E.; Schiessling, J.; Martensson, N.; Puglia, C. Scanning tunneling microscopy study of metal-free phthalocyanine monolayer structures on graphite. *J. Chem. Phys.* **2007**, *127*, 114702-114706.

[52] Lackinger, M.; Mueller, T.;Gopakumar, T.; Mu1ller, F.; Hietschold,M.; Flynn, G. W. Tunneling voltage polarity dependent submolecular contrast of naphthalocyanine on graphite. A STM study of close-packed monolayers under ultrahigh-vacuum conditions. *J. Phys. Chem. B* 2004, *108*, 2279-2284.

[53] Petraki, F.; Peisert, H.; Biswas, I.; Chasse, T. Electronic structure of Co-phthalocyanine on gold investigated by photoexcited electron spectroscopies: Indication of Co ion-metal interaction. *J. Phys. Chem. C* **2010**, *114,* 17638-17643.

[54] Petraki, F.; Papaefthimiou, V.; Kennou1, S. A study of the Ni-Phthalocyanine/gold interface using X-Ray and ultraviolet photoelectron spectroscopies. *J. Phys.: Conf. Ser.* **2005**, *10*, 135-138.

[55] Guo, Q.; Zang, K.; Liu, C.; Qin, Z.; Yu, Y.; Cao, G. Coverage-dependent structures of cobalt-phthalocyanine molecules adsorbed on Cu(001) surface. *Langmu*ir **2010**, *26*, 11804-11808.

[56] Lei, S.-B.; Deng, K.; Yang, D.-L.; Zeng, Q.-D.; Wang, C. Charge-transfer effect at the interface of phthalocyanine-electrode contact studied by scanning tunneling spectroscopy. *J. Phys. Chem. B* **2006***, 110*, 1256-1260.

[57] Toader, M.; Gopakumar, T. G.; Shukrynau, P.; Hietschold, M. Exploring the F_{16}CoPc/Ag(110) interface using scanning tunneling microscopy and spectroscopy. 2. Adsorption-induced charge transfer effect. *J. Phys. Chem. C* **2010**, *114,* 21548-21554.

[58] Takada, M.; Tada, H. Scanning tunneling microscopy and spectroscopy of phthalocyanine molecules on metal surfaces. J*apan. J. Appl. Phys.* **2005***, 44*, 5332-5335.

[59] Murdey, R.; Sato, N.; Bouvet, M. Frontier electronic structures in fluorinated copper, phthalocyanine thin films studied using ultraviolet and inverse photoemission spectroscopies. *Mol. Cryst. Liq. Cryst.* **2006**, *455*, 211–218.

[60] Lever, A. B. P. Derivation of metallophthacyanine redox potentials via Hammett parameter analysis. *Inorg. Chim. Acta* **1993**, *203*, 171-174.

[61] Takahata, Y.; Chong, D. P. Estimation of Hammett sigma constants of substituted benzenes through accurate density-functional calculation of core-electron binding energy shifts. *Inter. J. Quant. Chem.* **2005**, *103*, 509-515.

[62] Golovin, M. N.; Seymour, P.; Jayaraj, K.; Fu, Y.-S.; Lever, A. B. P. Perchlorinated phthalocyanines: Spectroscopic properties and surface electrochemistry. *Inorg. Chem.* **1990,** *29,* 1719-1727**.**

[63] Claußen, J. A.; Ochoa, G.; Páez, M.; Costamagna, J.; Gulppi, M.; Nyokong, T.; Bedioui, F.; Zagal, J. H. Volcano correlations for the reactivity of surface-confined cobalt N4-macrocyclics for the electrocatalytic oxidation of 2-mercaptoacetate. *J. Solid State Electrochem.* **2008**, *12*, 473-481.

[64] Sommerauer, M.; Rager, C.; Hanack, M. Separation of 2(3),9(10),16(17),23(24)-tetrasubstituted phthalocyanines with newly developed HPLC phases. *J. Am. Chem. Soc.* **1996**, *118,* 10085-10093.

FIGURE CAPTIONS

Figure 1. Molecular structure of phthalocyanine tetrasulfonic acid. TSPc has several regioisomers. Atom labels on the molecule refer to specific nitrogens in the XPS assignments discussed in this work.

Figure 2. Absorption spectra (coded in color) of 10μM TSPc in water at pH 0 (black) adjusted with HCl. The red line spectrum is that of 10μM TSPc acquired in DMSO. This is a spectrum of monomeric phthalocyanine species presented here as a reference.

Figure 3. N1s region XPS for H_2Pc and TSPc powders and TSPc aggregates. The blue and red line fits in each spectrum are associated with the binding energies arising from the unprotonated and protonated Pc nitrogens, respectively. Black curve is a shake-up peak.

Figure 4. Large scale constant current STM image of TSPc aggregates on Au(111). Image was taken in UHV after heating the sample to 100º C. The set point was 1.6 V and 5 pA.

Figure 5. Representative UHV-STM images of TSPc aggregates formed on Au(111). Image (a) presents two types of self-organized structures: **1** parallel rows of TSPc molecules propagate down the length of the aggregate and **2** parallel lines of molecules are aligned at 60° to the long axis of the aggregate. In image (b) the parallel molecular rows form graduated steps. Both images were acquired after the samples were heated to 100 C. The set point was 1.6V and 5pA. Below each figure is a cross-section of a feature identified in the image.

Figure 6. Constant current high resolution image of a TSPc aggregate along with a cross-sectional view of molecular packing of the phthalocyanine. The sample was heated to 100 C in UHV before imaging. The molecular rows are 2 nm apart. The set point was 1.6V and 5pA.

Figure 7. Comparison of area averaged dI/dV spectra taken from a TSPc aggregate (red trace) with those obtained from monolayer films of CoPc (blue trace, reference 48) and VOPc (black

trace, reference 47) all on Au(111). The zeros of each trace are placed arbitrarily to allow easier comparison of spectra. Also shown is the *I/V* curve obtained from three layers of TSPc on Au(111).

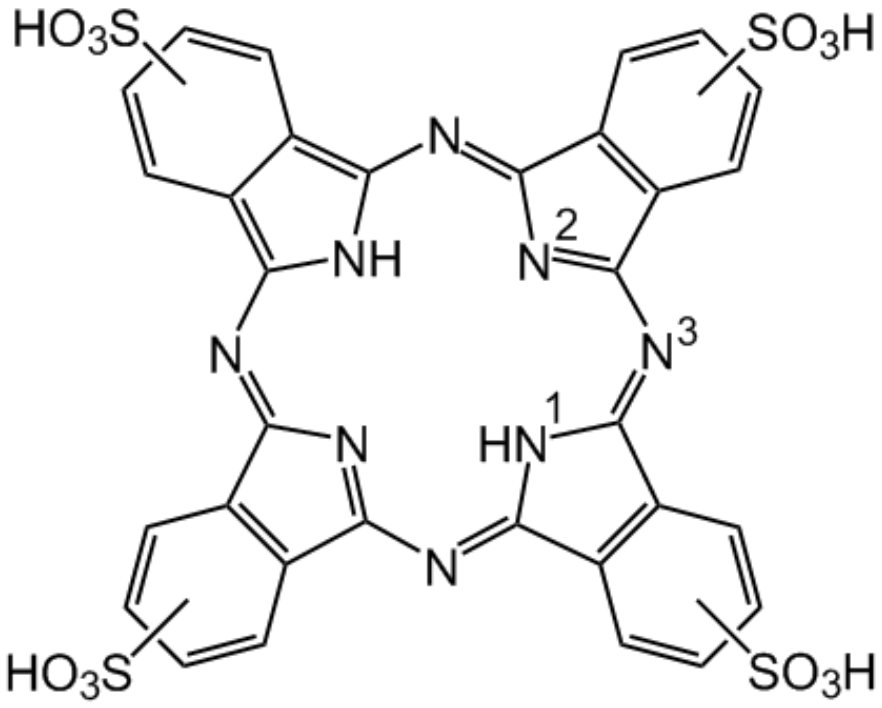

Figure 1. Molecular structure of phthalocyanine tetrasulfonic acid. TSPc has several regioisomers. Atom labels on the molecule refer to specific nitrogens in the XPS assignments discussed in this work.

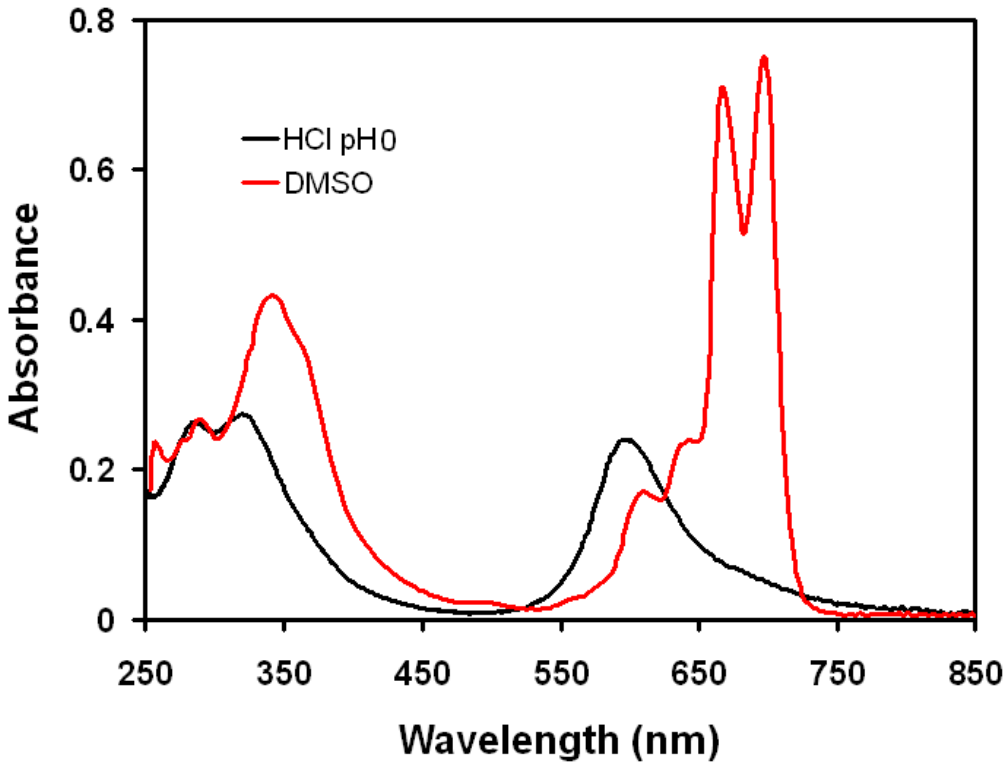

Figure 2. Absorption spectra (coded in color) of 10μM TSPc in water at pH 0 (black) adjusted with HCl. The red line spectrum is that of 10μM TSPc acquired in DMSO. This is a spectrum of monomeric phthalocyanine species presented here as a reference.

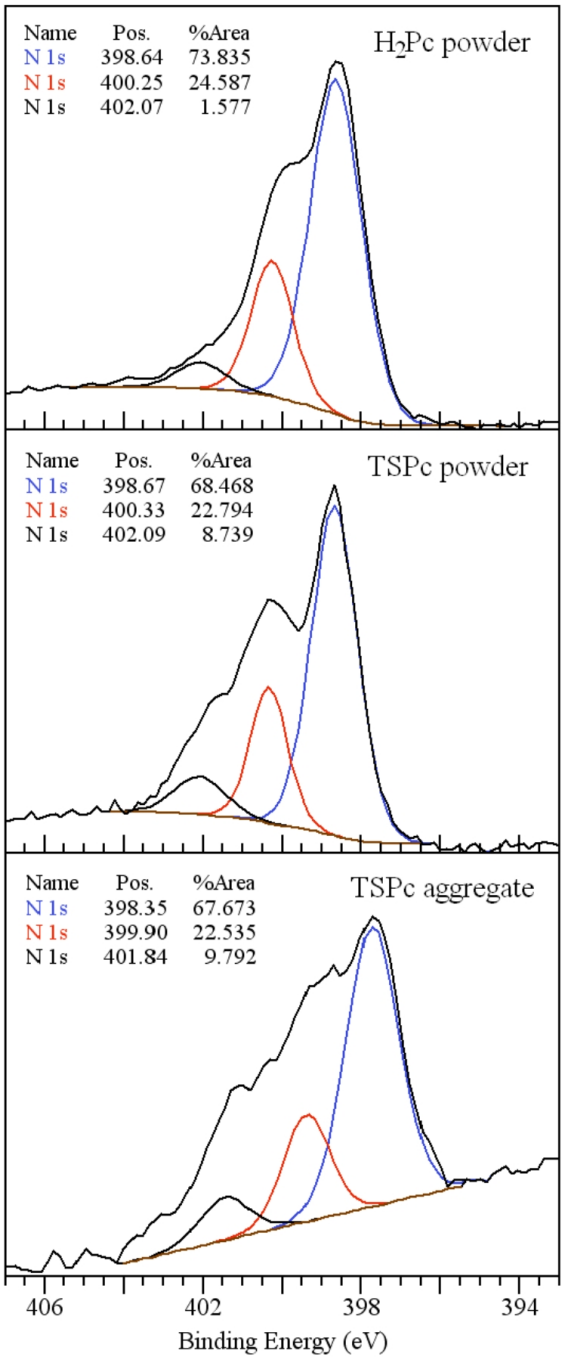

Figure 3. N1s region XPS for H_2Pc and TSPc powders and TSPc aggregates. The blue and red line fits in each spectrum are associated with the binding energies arising from the unprotonated and protonated Pc nitrogens, respectively. Black curve is a shake-up peak.

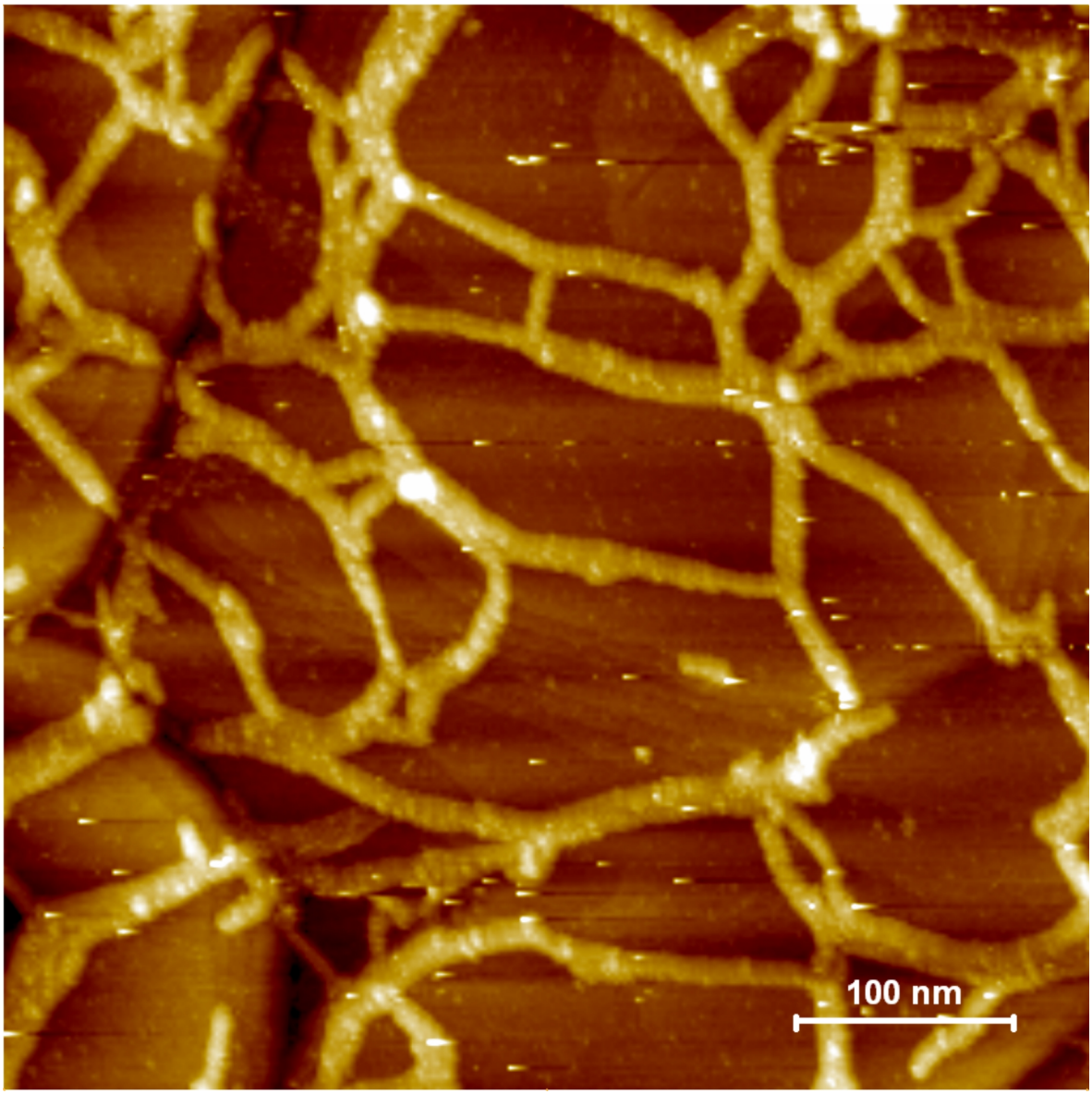

Figure 4. Large scale constant current STM image of TSPc aggregates on Au(111). Image was taken in UHV after heating the sample to 100º C. The set point was 1.6 V and 5 pA.

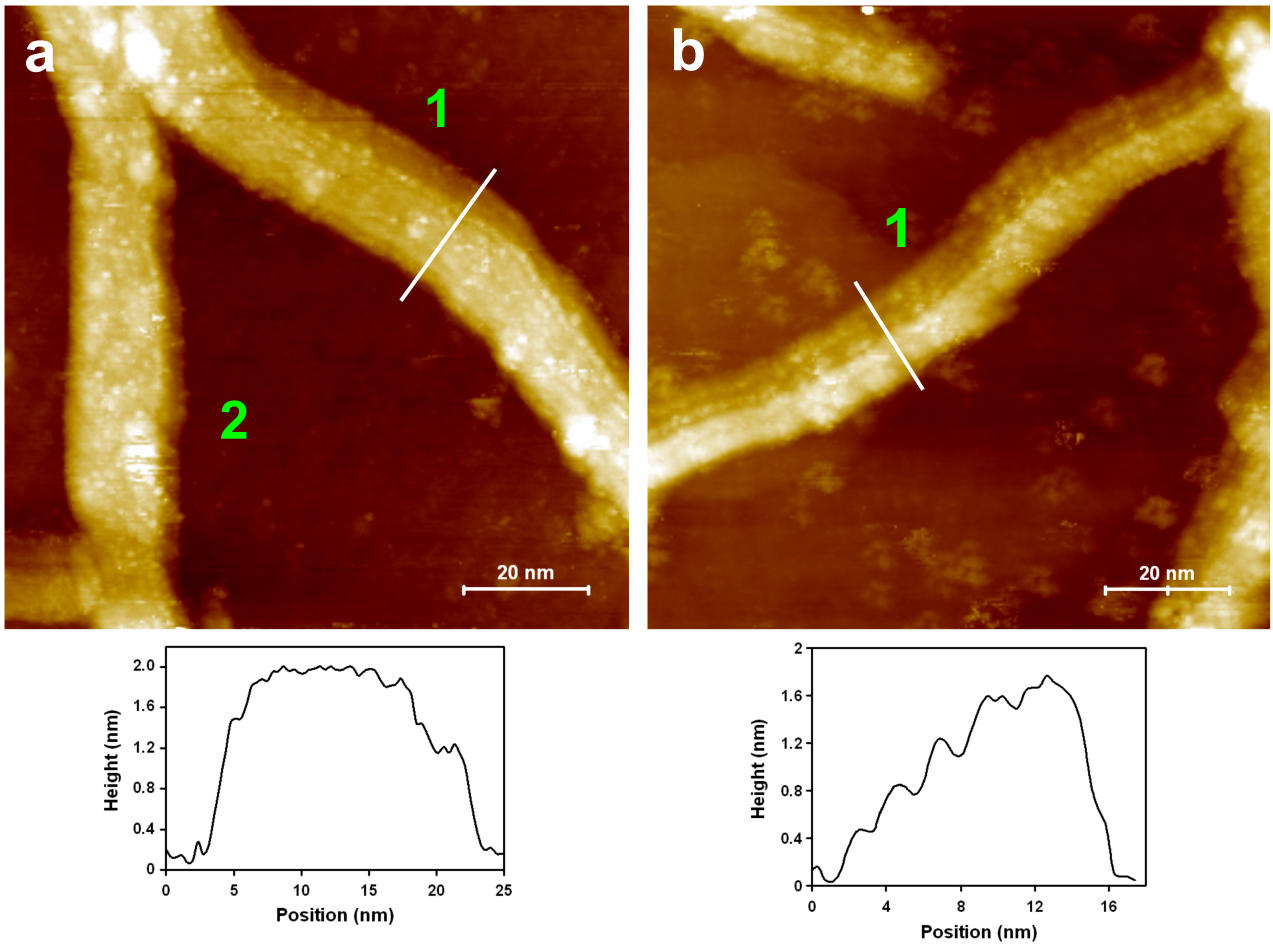

Figure 5. Representative UHV-STM images of TSPc aggregates formed on Au(111). Image (a) presents two types of self-organized structures: **1** parallel rows of TSPc molecules propagate down the length of the aggregate and **2** parallel lines of molecules are aligned at 60° to the long axis of the aggregate. In image (b) the parallel molecular rows form graduated steps. Both images were acquired after the samples were heated to 100 C. The set point was 1.6V and 5pA. Below each figure is a cross-section of a feature identified in the image.

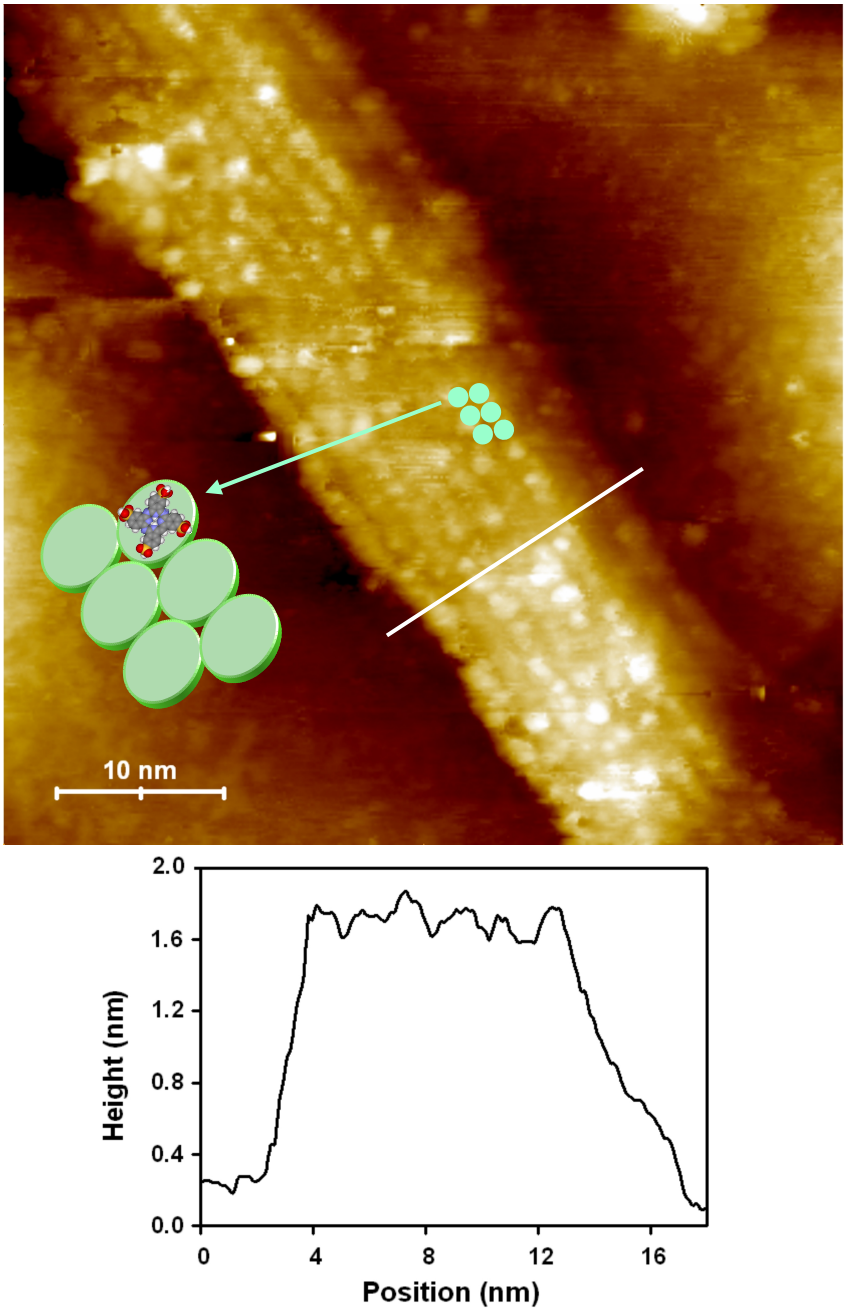

Figure 6. Constant current high resolution image of a TSPc aggregate along with a cross-sectional view of molecular packing of the phthalocyanine. The sample was heated to 100 C in UHV before imaging. The molecular rows are 2 nm apart. The set point was 1.6V and 5pA.

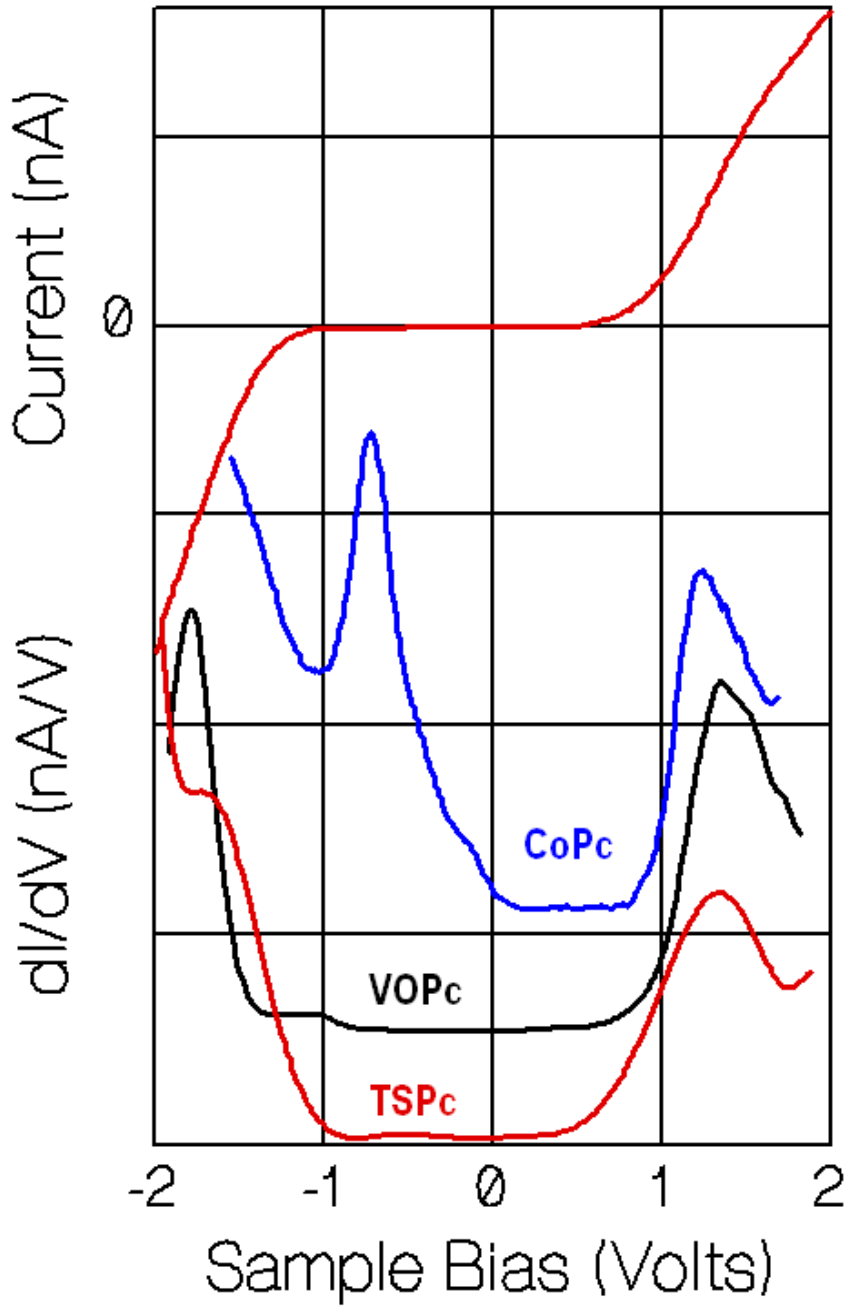

Figure 7. Comparison of area averaged d*I*/d*V* spectra taken from a TSPc aggregate (red trace) with those obtained from monolayer films of CoPc (blue trace, reference 48) and VOPc (black trace, reference 47) all on Au(111). The zeros of each trace are placed arbitrarily to allow easier comparison of spectra. Also shown is the *I*/*V* curve obtained from three layers of TSPc on Au(111).

TOC Graphic